TR 70090

MAY

1970

ROYAL AIRCRAFT ESTABLISHMENT

TECHNICAL REPORT 70090

ON CONICAL WAVERIDERS

by

J. Pike

MINISTRY OF TECHNOLOGY
FARNBOROUGH HANTS

CONTENTS

U.D.C. 533.692.55 : 533.696.4 : 533.6.011.72 : 533.6.011.5

ROYAL AIRCRAFT ESTABLISHMENT

Technical Report 70090

May 1970

ON CONICAL WAVERIDERS

by

J. Pike

SUMMARY

Conical flow fields in which details of the flow are known, are used to produce lifting surfaces which are conical about their 'noses' and concave, nearly flat or convex across their span.

At the appropriate Mach number (i.e. 3.53 or 4 for this Report), the flow about the surfaces is known, and it is found that surfaces intermediate in shape between the flat delta and the caret wing have lift-to-drag ratios better than either.

Departmental Reference: Aero 3108

1 INTRODUCTION

Supersonic lifting surfaces with theoretically predictable pressure distributions have been obtained by replacing stream surfaces in known flow fields with solid surfaces. Previously this method has been applied to two-dimensional[1,2] and axisymmetric[3] flow fields; here it is applied to conical flow fields, resulting in a new range of lifting surfaces with known pressure distributions.

Only conical compression surfaces are considered in detail in this Report however conical flow fields can yield compression surfaces which are not conical. For example, such compression surfaces (from the flow about an unyawed cone) have been obtained by Jones[4]. The lift to drag ratios which could be obtained from these non-conical surfaces are investigated using the momentum method of Roe[5].

Conical compression surfaces for which exact descriptions of the flow have been obtained previously are those of the caret wing[1,2] and the flat delta wing[7]. The lift to pressure drag ratio of the caret compression surface is the same as that of a plane two-dimensional wedge with the same lift coefficient. However, the larger wetted area of the caret wing can significantly reduce its overall lift to drag ratio compared with that of the wedge. Typically if $M < 2/(s/\ell)$ then the lift to drag ratio is 5% less than that of the wedge, and if $M < 1.2/(s/\ell)$ the reduction becomes 10% or more[6]. In contrast, the lift to pressure drag ratio of the flat delta compression surface is typically 2 - 3% less than that of the wedge[7], but its wetted area is small such that it is not at any further disadvantage when friction drag is included. It has been suggested[8] that compression surfaces of the same (delta) planform but intermediate in concavity between the caret and the flat delta, can have lift to drag ratios better than the caret (or the wedge) and wetted areas little more than that of the flat delta (or the wedge). Such compression surfaces are found amongst the conical compression surfaces investigated here; they have lift to drag ratios better than both the caret and flat delta values.

Although the examples presented here are restricted by the flow fields available[9-12] to Mach numbers of 3.53 and 4, at higher Mach numbers (where the lift to drag ratio tends to be less sensitive to spanwise changes in shape) similar results must be expected to hold. Conical compression surfaces at higher Mach numbers will be produced when the flow fields of sufficient detail become available.

2 CONICAL FLOW FIELDS AND COMPRESSION SURFACES

The steady inviscid supersonic flow past a conical body (Fig.1) can be described by partial differential equations in two variables. These equations have been solved numerically[9-12] to produce several flows which contain conical stream surfaces. By replacing these stream surfaces with solid surfaces we can obtain conical compression surfaces with known flow about them. Two simple examples of conical flow fields are those which are also axisymmetric or two-dimensional. Fig.2 shows the side view and a section normal to the free stream direction, through the axisymmetric flow about an unyawed circular cone. The conical stream surfaces are planes ϕ = constant (in polar co-ordinates r, θ, ϕ). In this flow, replacing the stream surfaces (ss) with a solid surface gives the flow past a half cone beneath a delta wing.

The two dimensional flow past an unyawed wedge supporting a plane inclined shock wave is shown in side view and section in Fig.3. The conical centre (O) is at any point on the shock wave. The free stream direction (OX) and the flow direction behind the shock wave (OY) are shown. The conical stream surfaces are planes passing through OY, which when replaced by solid surfaces give the well known caret wing compression surfaces[1,2]. If viscous effects are neglected, the lift to drag ratio of these surfaces is the same as that of the original wedge (i.e. L/D = cot α), and they provide a convenient basis on which to compare the inviscid performance of other compression surfaces. The conical compression surfaces produced here are compared with caret wings which have the same planform and, with the upper surface streamwise, either the same lift coefficient, or the same volume.

The ratio of wetted area to planform area is important in determining the skin friction drag. For the wedge surface it is close to unity; for the caret wing at low supersonic Mach numbers it tends to be large. The wetted area to planform area of the conical wings is compared with both wedge and caret wing values.

In Fig.4, the flow about a yawed circular cone at M = 3.53 is shown[10]. Conical stream surfaces (shown dotted) can again be chosen to represent compression surfaces. All these conical surfaces converge on a line on the cone surface at Y. The shock wave strength is not constant for the yawed cone; hence the streamlines converging on Y have different entropies, and large entropy gradients occur close to Y[13]. In real flows these entropy gradients

are reduced by viscous effects. This could cause significant changes in the flow of the complete flow field. Here, as only a part of the flow field is used over which the shock wave strength does not vary greatly, the inclusion of viscosity would produce small changes, which are neglected along with those from the boundary layer.

Figs.5 and 6 show conical wings with streamwise upper surfaces, and lower surfaces produced from the flow about circular cones of 20° semi-angle, yawed at 5° and 10° respectively. The plan and side views in these figures are shown to a smaller scale than the front views. The shapes are all conical and therefore the front view also depicts any section. The shock wave and pressure distribution for the section are also shown. Below each example the values of the following parameters are indicated:-

C_L : lift coefficient

C_D : pressure drag coefficient

L/D_p : lift over pressure drag

s/ℓ : semi-span to length ratio

τ : volume parameter $\{\text{Volume}/(\text{Plan Area})^{3/2}\}$

S_w/S : ratio of wetted area to plan area for the compression surface

E_p : ratio of L/D_p to that of a caret wing with the same C_L

E_τ : ratio of L/D_p to that of a caret wing with the same planform and volume

R_w : ratio of S_w/S for the wing shown, to that for a caret wing with the same planform and C_L

The incidence of the wings shown in Fig.5 is such as to give large values of lift coefficient and small values of lift to drag ratio. In Fig.6, the increased yaw of the cone producing the flow field results in wings with smaller lift coefficients and higher lift to drag ratios. A similar result could have been achieved by retaining 5° of yaw and reducing the cone apex angle.

In Fig.7 conical compression surfaces from the flow about an elliptic cone[11] are shown. The lift coefficient is small for these surfaces and the resulting lift to pressure drag ratios high.

In Figs.5 to 7 a wide range of values of s/ℓ are shown. Wings of small s/ℓ have high τ and a large ratio of wetted area to planform area. The inviscid

performance is very close to that of the caret wing whether compared on a lifting (E_p) or a volume (E_τ) basis. However the wetted area is considerably less than that of the caret wing (see R_w); hence the performance in viscous flow would be better than that of the caret wing with the same planform and C_L or τ.

For the nearly flat surfaces (S_w/S-1) with friction drag included, the lift to drag ratio is close to that of the flat two-dimensional surface with the same planform.

3 LIFT TO DRAG RATIO INVESTIGATIONS USING MOMENTUM METHODS

The lift to drag ratios of the conical compression surfaces produced in Section 2, are at best little better than those of the appropriate plane two-dimensional wedge. However the examples of Section 2 are all conical, and it is not clear that non-conical surfaces from conical flow fields will not have considerably improved performance. By Roe's method[5] the lift to pressure drag ratio of all the surfaces which may be obtained from a particular flow field, can be assessed by investigating the lift and drag of individual streamtubes.

As the lift and drag of any surface is formed from the sum of these incremental lifts and drags, it is possible to make predictions about any surface obtainable from the flow field by inspecting the streamtube values.

For the streamtubes in the flow about the cone with 10^o of yaw, Fig.8(a) shows contours for constant values of lift function (i.e. non-dimensional lift); in Fig.8(b) the conical stream surfaces used to produce the wings of Fig.6 are shown. The correlation between the increasing lift coefficient of the compression surfaces 'a' to 'e' and the increasing value of the lift function over the regions YaP, YbP, YcP, YdP and YeP demonstrates how the lift coefficients of the surfaces are influenced by the value of the lift function.

The lift function over drag function contours in the base plane are shown in Fig.8(c). They tend to follow the lift function contours, low lift giving high lift to drag ratio and vice-versa. More interesting is the comparison of these values with the values from a streamtube with the same lift function in the flow about a plane two-dimensional wedge; for to produce compression surfaces which are better than the wedge, we at least need to include streamtubes in the flow which have locally better lift to drag ratios than the wedge.

The value of the lift over drag function when compared with the wedge value for the same lift function is a type of flow efficiency parameter (E).

E values for the 10^{o} yawed cone flow are shown in Fig.8(d) to vary from 1.7 to 0.6.

By superimposing the stream surfaces of Fig.8(b) on 8(d) we see that as more of the efficient region near E = 1.7 is included in the region between the surface and the shock wave, so is more of the inefficient region near E = 0.6. Further, for shapes which are near flat at the base, the efficient region of the flow inboard is always compensated by inefficient flow outboard, which gives an overall lift to pressure drag ratio near to the wedge value. The inefficient region outboard could be reduced in extent by increasing the anhedral of the tips of a wing such as (d) of Fig.6 (or 8(b)). However to make any significant difference to the lift to drag ratio, the wetted area to plan area would have to be increased so much that the inclusion of friction drag would tend to reduce the lift to drag ratio to a value close to that of the wedge.

4 CONCLUSIONS

A number of conical wings with curved compression surfaces are derived in such a way that surface pressure, shock wave shape and force coefficients are known for a particular incidence and Mach number (i.e. M = 3.53 or 4). It is found that even though the available ranges of semispan to length ratio, anhedral angle and lift coefficient are considerable, the ratios of lift to pressure drag are consistently close to the caret wing value whether compared on a lift coefficient or a volume basis. When viscous drag is included, the smaller wetted areas of the conical wings evaluated here, compared with those of equivalent carets, give the conical wings an overall lift to drag ratio better than the caret values.

Conical compression surfaces which are nearly flat have lift to drag ratios very close to those of the flat two-dimensional wedge. Some wings with small anhedral are found which have lift to drag ratios slightly better than the wedge values. Thus from conical flow fields can be obtained simple conical wings with known flow at a particular Mach number, good lift to drag ratio[6] and an anhedral angle smaller than that of the caret wing with a similar semi-span to length ratio.

By use of Roe's[5] momentum theory, it is found that non-conical shapes from the flow field would be restricted at best to having lift to drag ratios close to those of the wedge.

ACKNOWLEDGMENT

The author wishes to thank F. E. Manger for supplying the yawed cone flow field data, and B. A. L. Hart for supplying the elliptic cone flow field data used in this Report.

LIST OF SYMBOLS

C_D	pressure drag coefficient
C_L	lift coefficient
E	ratio of the lift over drag function for a streamtube, to that for a streamtube in a wedge flow with the same lift function
E_p	ratio of L/D_p to that of a caret wing with the same C_L
E_τ	ratio of L/D_p to that of a caret wing with the same planform and volume
L/D_p	lift over pressure drag
L/D	lift over (pressure + viscous drag)
R_w	ratio of S_w/S for the wing shown, to that for a caret wing with the same planform and C_L
s/ℓ	ratio of semi-span to length
S_w/S	ratio of wetted area to plan area
τ	volume parameter, $\{\text{Volume}/(\text{Plan area})^{3/2}\}$

REFERENCES

No.	Author	Title, etc.
1	T. R. F. Nonweiler	Aerodynamic problems of space vehicles. J.R.Ae. Soc 63 (585) (1959)
2	T. R. F. Nonweiler	Delta wings of shapes amenable to exact shock wave theory. ARC 22644 March 1961 J.R.Ae. Soc 67 (625) (1963)
3	J. G. Jones K. C. Moore J. Pike P. L. Roe	A method for designing lift configurations for high supersonic speeds using axisymmetric flow fields. Ingenieur-Archiv, 37. Band, 1. Heft, 1968, S.56-72
4	J. G. Jones B. A. Woods	The design of compression surfaces for high supersonic speeds using conical flow fields. A.R.C. R & M 3539 (1963)
5	P. L. Roe	A momentum analysis of lifting surfaces in inviscid supersonic flow. R.A.E. Technical Report 67124, ARC 29530, R & M 3576
6	J. Pike	On the maximum lift to drag ratio of wings at high supersonic speeds. R.A.E. Technical Report to be published.
7	D. A. Babaev	Numerical solution of the problem of supersonic flow past the lower surface of a delta wing. Zhurnal Vychislitel'noi Matematiki i Matematicheskoi Fiziki 2, No.6, 1086-1101 (1962)
8	J. Pike	The flow past flat and anhedraled delta wings with attached shock waves. R.A.E. Technical Report to be published.
9	B. P. Briggs	Calculation of supersonic flow past bodies supporting shock waves shaped like elliptic cones. NASA Report D-24 (1959)

REFERENCES (contd)

No.	Author	Title, etc.
10	P. M. Stocker F. E. Mauger	Supersonic flow past cones of general cross-section. J. Fluid Mechanics 13, 383 (1962)
11	F. Walkden B. A. L. Hart	Supersonic flow fields produced by conical bodies of arbitary cross-section. R.A.E. Report 66129 (1966)
12	R. Gonidou	Ecoulements supersoniques autour de cônes en incidence. La Recherche Aerospatiale no 120 (1967)
13	J. H. B. Smith	Remarks on the structure of conical flow. R.A.E. Technical Report 69119, ARC 31506 (1969)

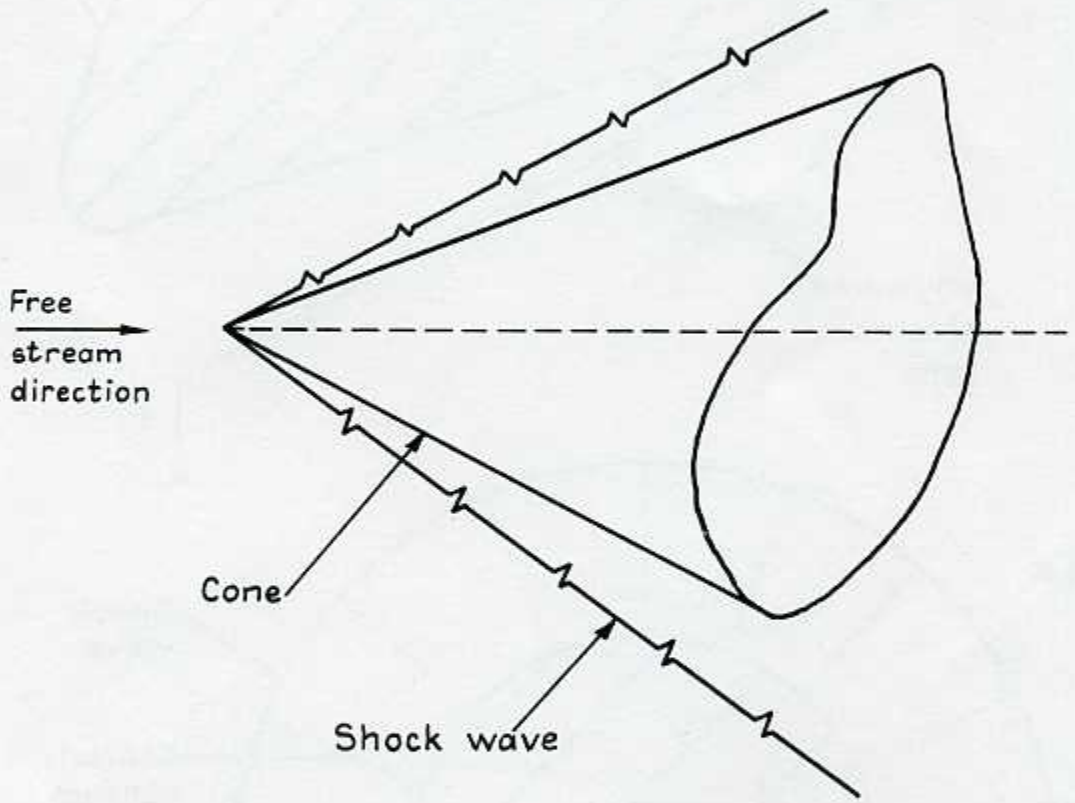

Fig. 1 Steady inviscid supersonic flow past a conical body

Fig. 2

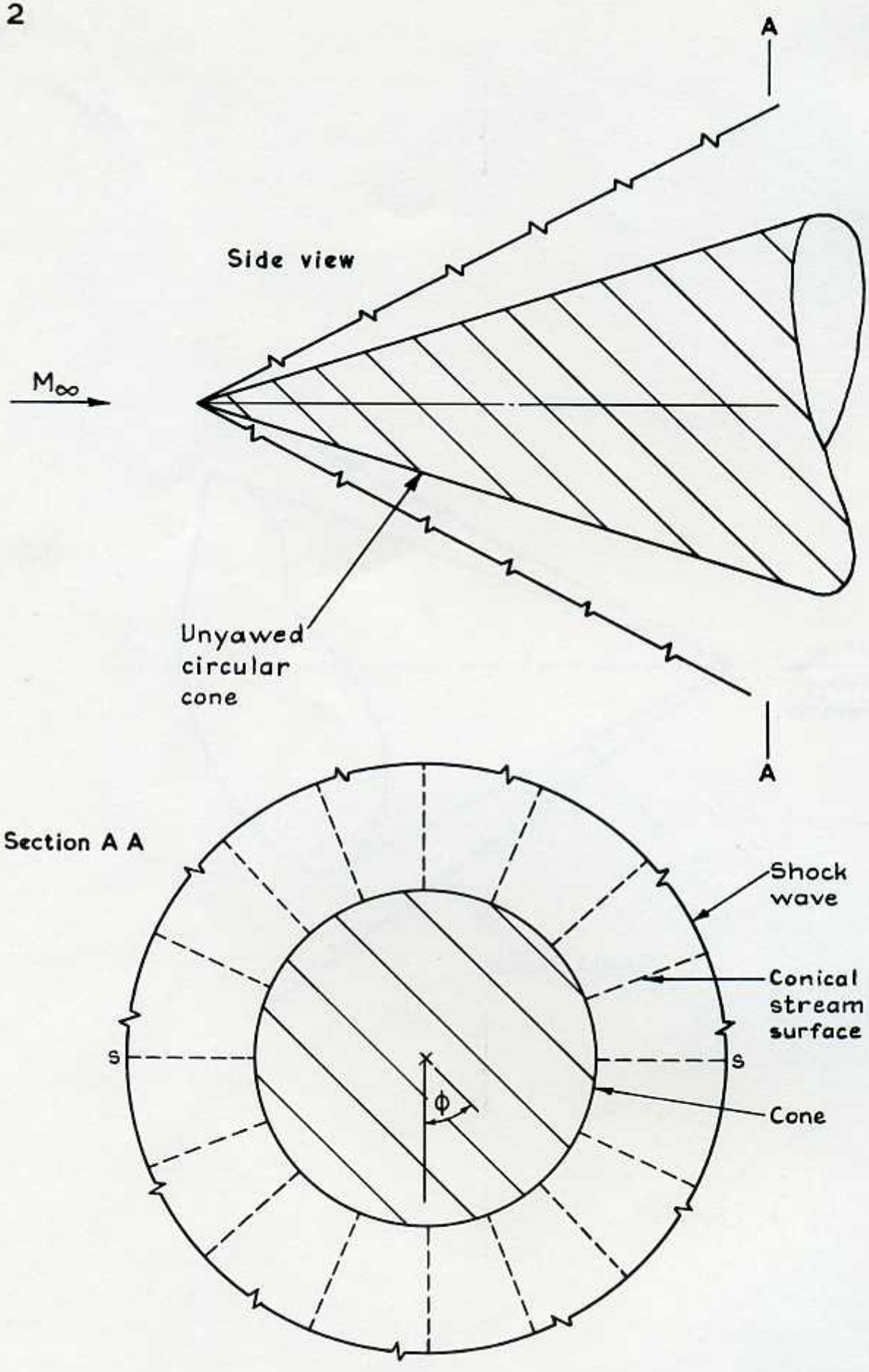

Fig. 2 Conical stream surfaces behind a shock wave shaped like a circular cone

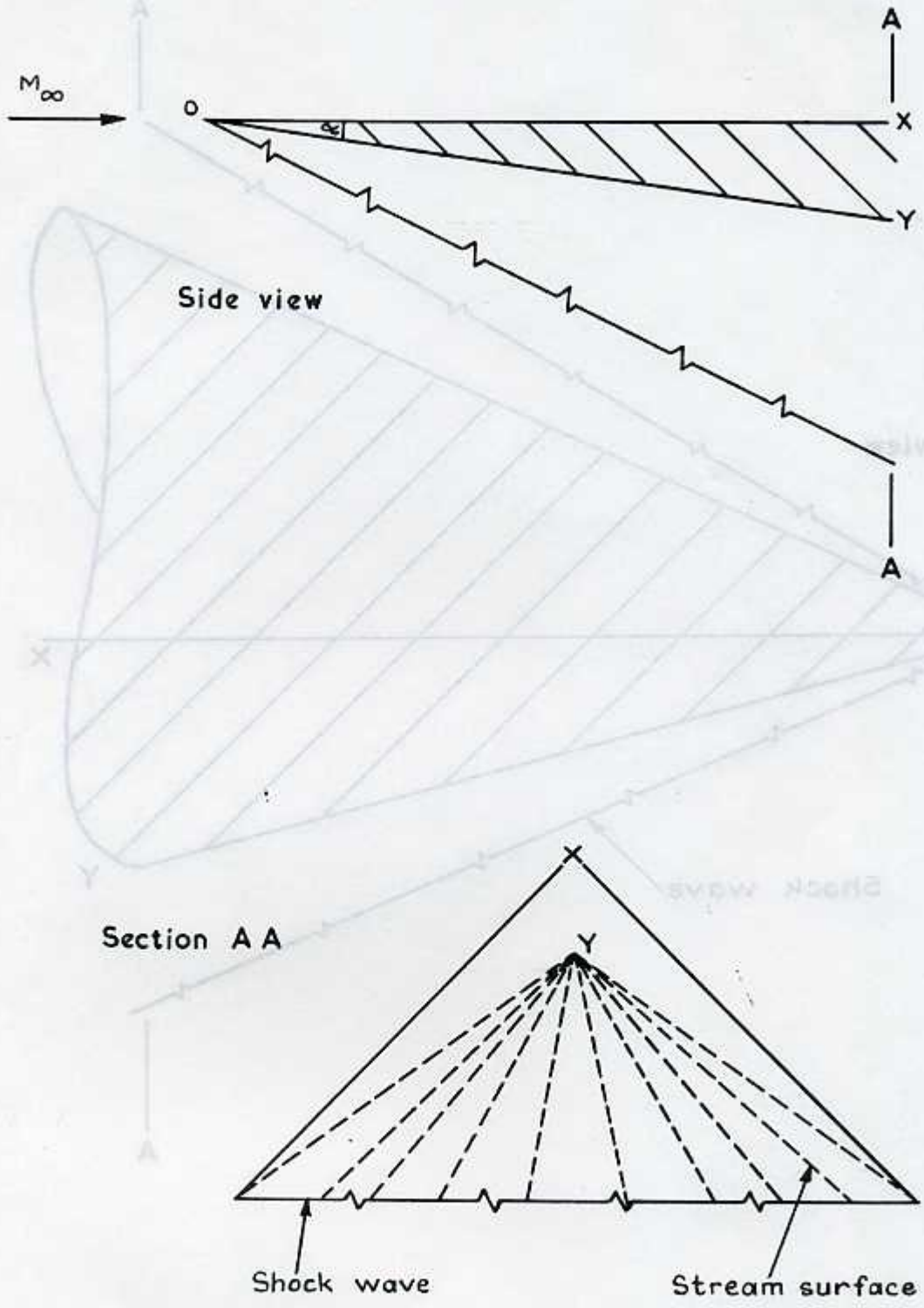

Fig. 3 Conical stream surfaces behind a plane shock wave

Fig. 4

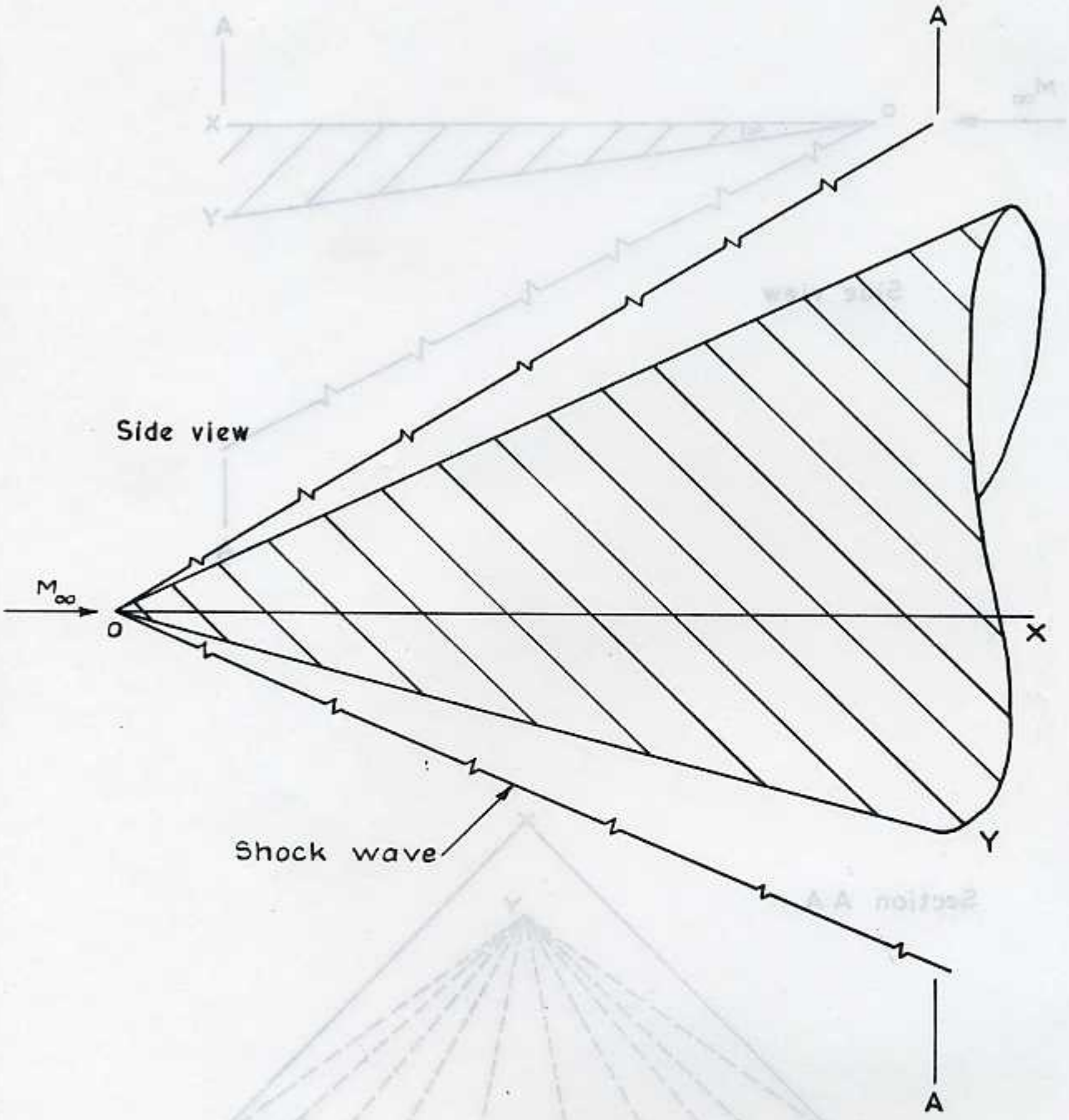

Fig. 4 Conical stream surfaces in a M=3·53 flow past a yawed circular cone
(see facing page)

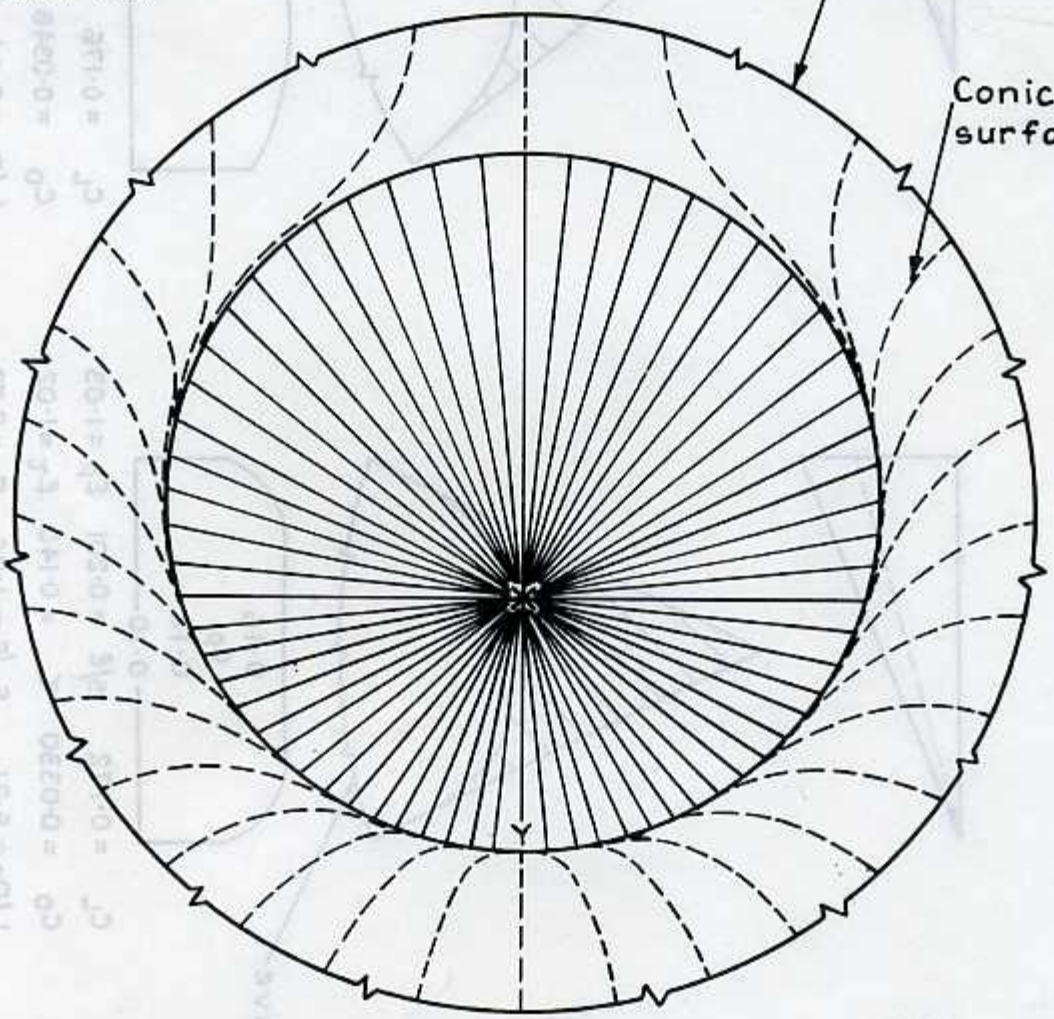

Fig. 4 contd

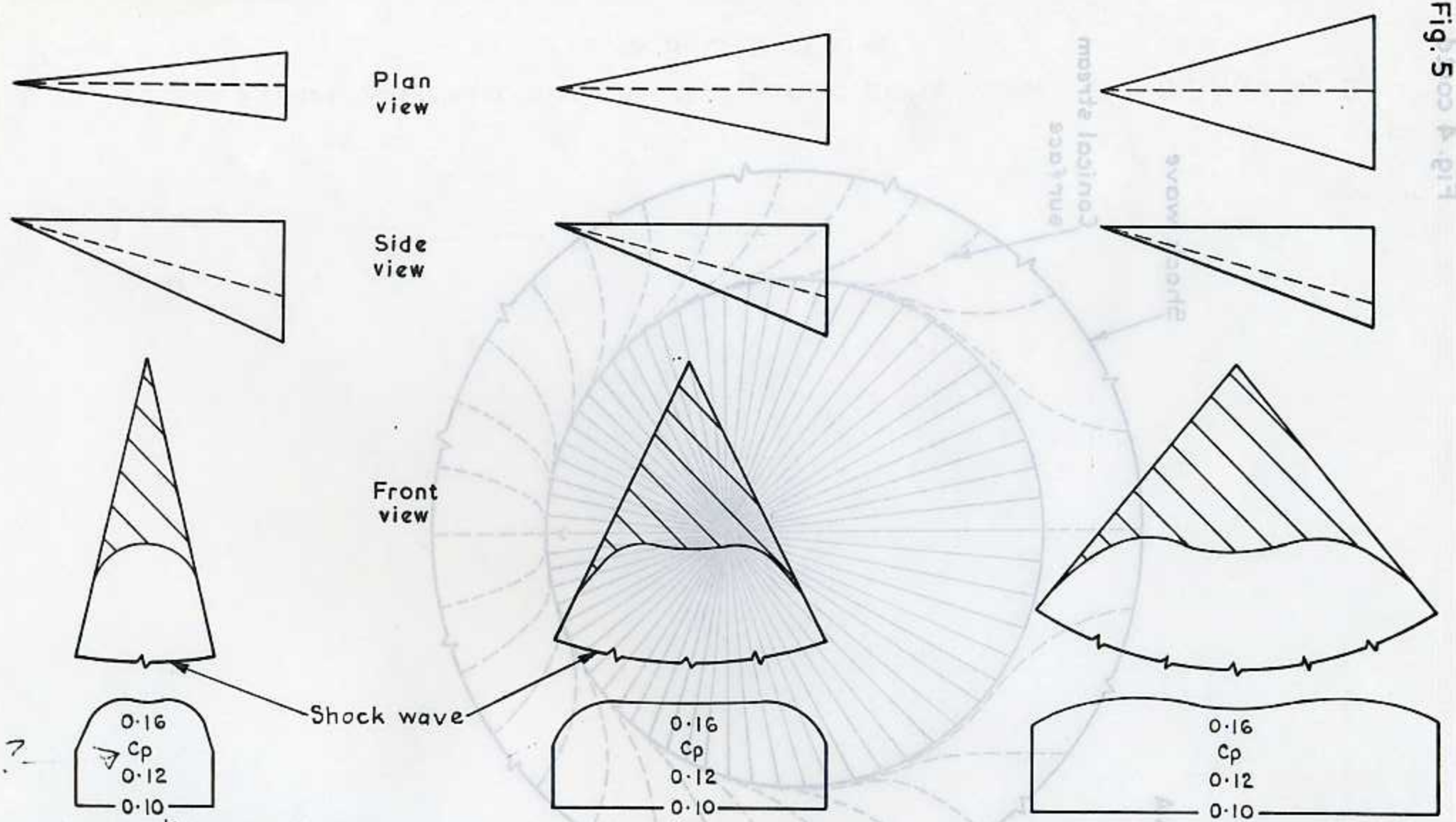

C_L = 0·169 s/ℓ = 0·102 E_p = 1·03
C_D = 0·0322 τ = 0·194 E_τ = 1·02
L/D_p = 5·26 S_w/S = 2·16 R_w = 0·75

C_L = 0·172 s/ℓ = 0·201 E_p = 1·03
C_D = 0·0330 τ = 0·140 E_τ = 1·02
L/D_p = 5·21 S_w/S = 1·36 R_w = 0·79

C_L = 0·176 s/ℓ = 0·292 E_p = 1·02
C_D = 0·0348 τ = 0·121 E_τ = 1·01
L/D_p = 5·04 S_w/S = 1·13 R_w = 0·81

Fig. 5 Waveriders from 20° circular cone with 5° yaw at M=3·53

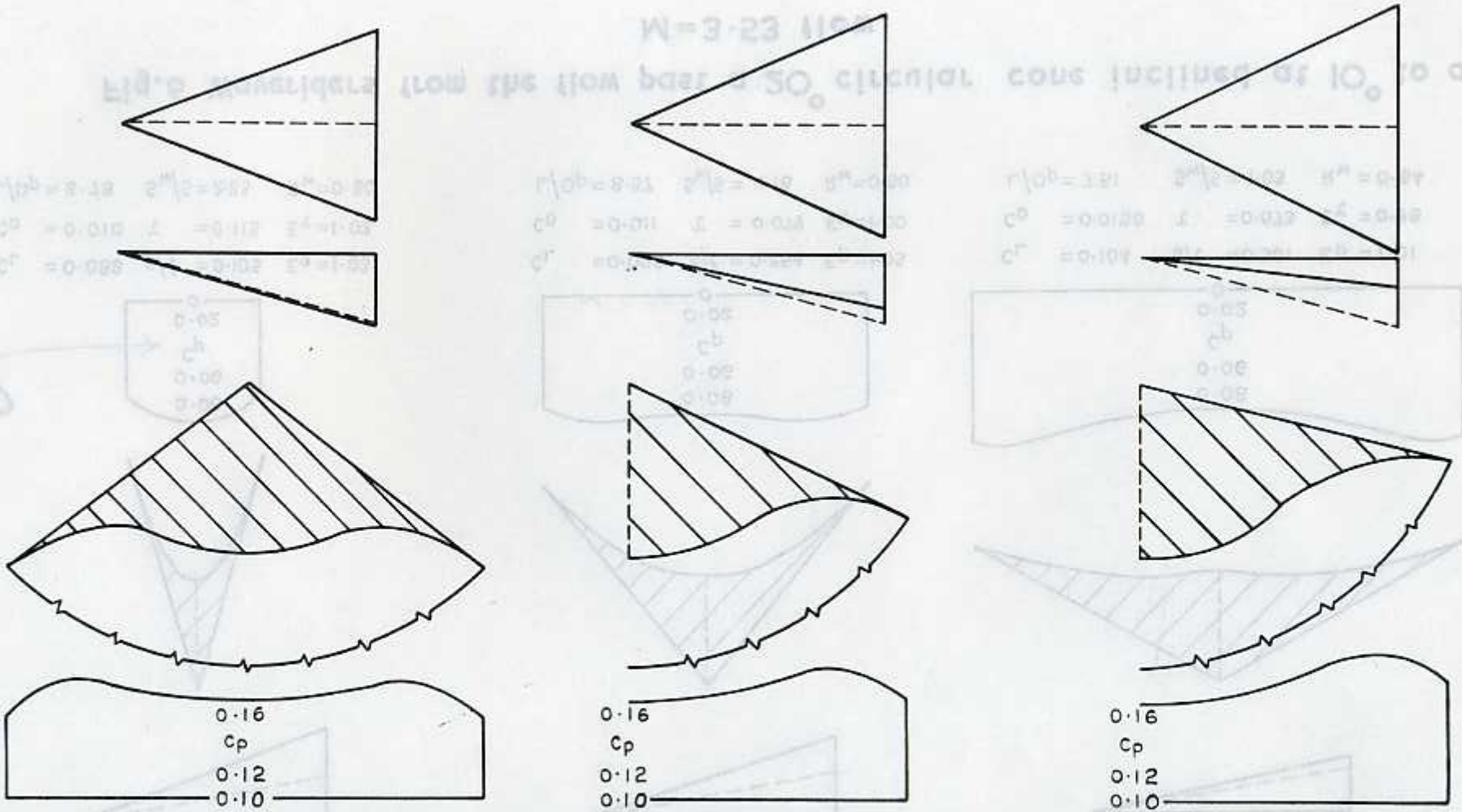

C_L = 0·181 s/ℓ = 0·372 E_p = 0·99
C_D = 0·0378 τ = 0·114 E_τ = 1·00
L/D_p = 4·79 S_w/S = 1·07 R_w = 0·85

C_L = 0·187 s/ℓ = 0·437 E_p = 0·94
C_D = 0·0420 τ = 0·114 E_τ = 0·99
L/D_p = 4·46 S_w/S = 1·08 R_w = 0·90

C_L = 0·194 s/ℓ = 0·486 E_p = 0·88
C_D = 0·119 τ = 0·119 E_τ = 0·99
L/D_p = 4·06 S_w/S = 1·13 R_w = 0·96

Fig. 5 contd Waveriders from the flow past a 20° circular cone inclined at 5° to a M=3·53 flow

Fig. 5 contd

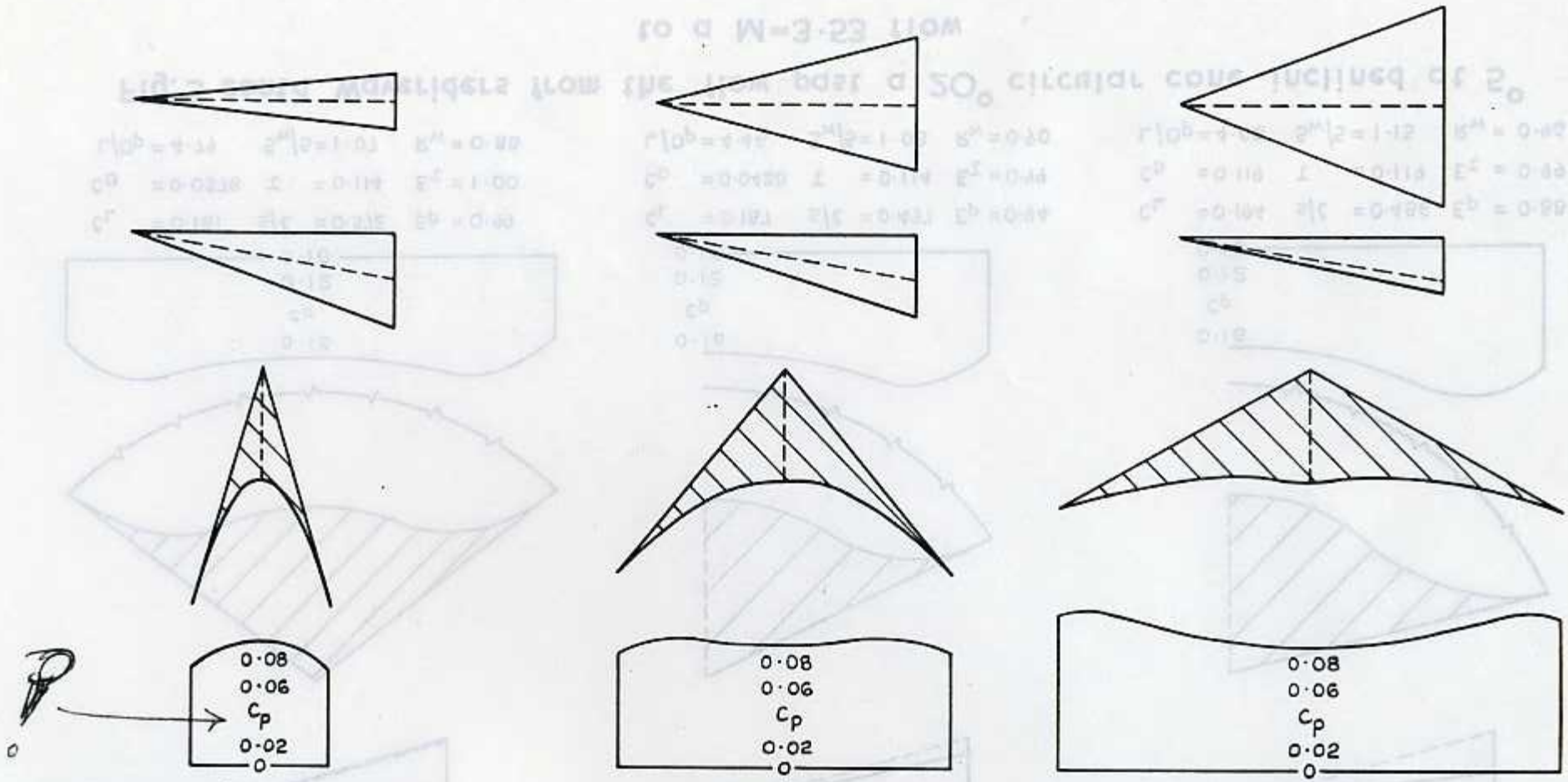

C_L = 0·088	s/ℓ = 0·105	E_p = 1·03
C_D = 0·010	τ = 0·115	E_τ = 1·02
L/D_p = 8·78	S_w/S = 2·23	R_w = 0·80

C_L = 0·093	s/ℓ = 0·254	E_p = 1·03
C_D = 0·011	τ = 0·079	E_τ = 1·00
L/D_p = 8·37	S_w/S = 1·18	R_w = 0·80

C_L = 0·104	s/ℓ = 0·381	E_p = 1·01
C_D = 0·0138	τ = 0·073	E_τ = 0·98
L/D_p = 7·51	S_w/S = 1·03	R_w = 0·84

Fig. 6 Waveriders from the flow past a 20° circular cone inclined at 10° to a M = 3·53 flow

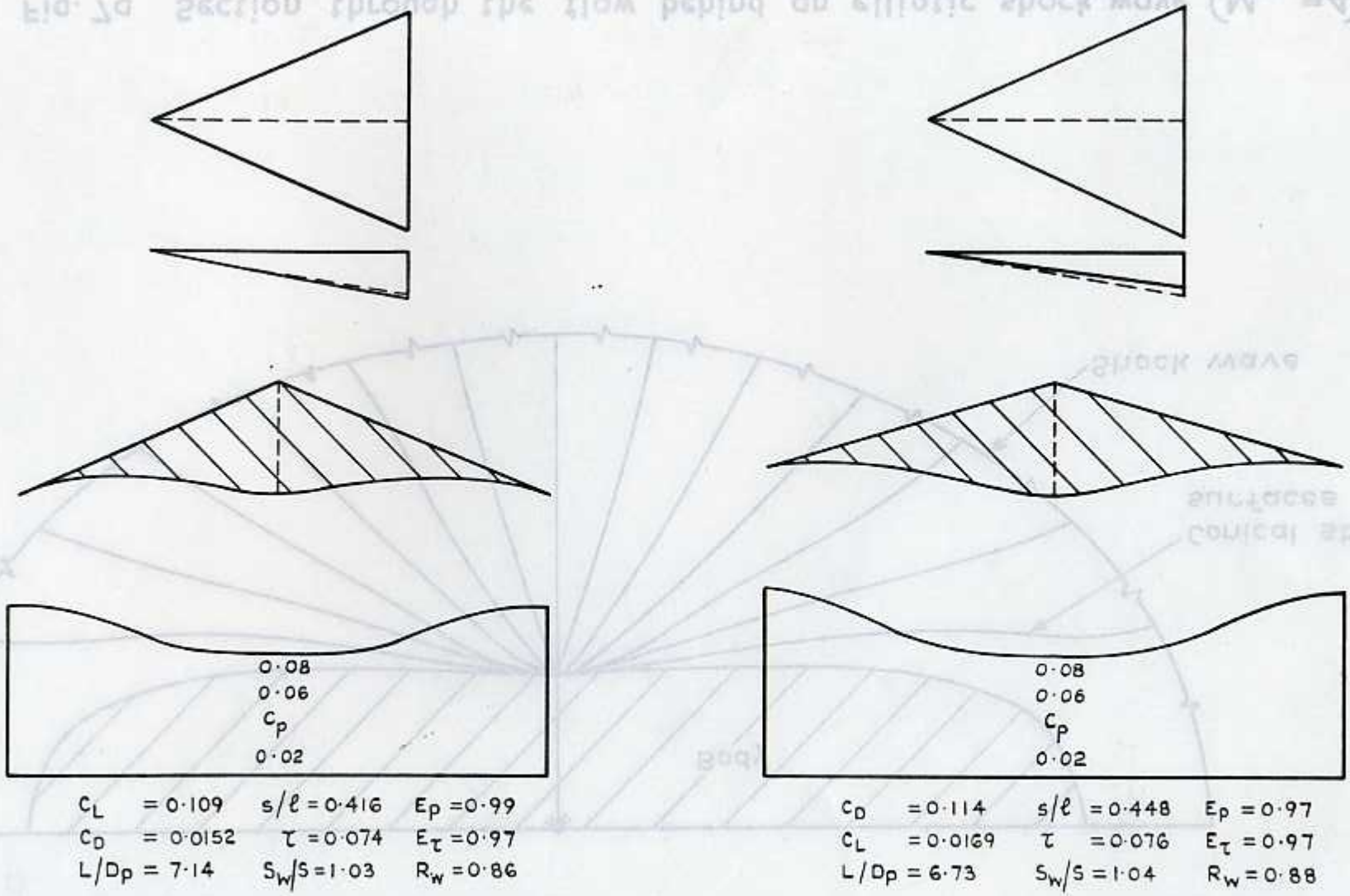

Fig. 6 contd Waveriders from the flow past a 20° circular cone inclined at 10° to a M=3·53 flow

Fig.6 d&e

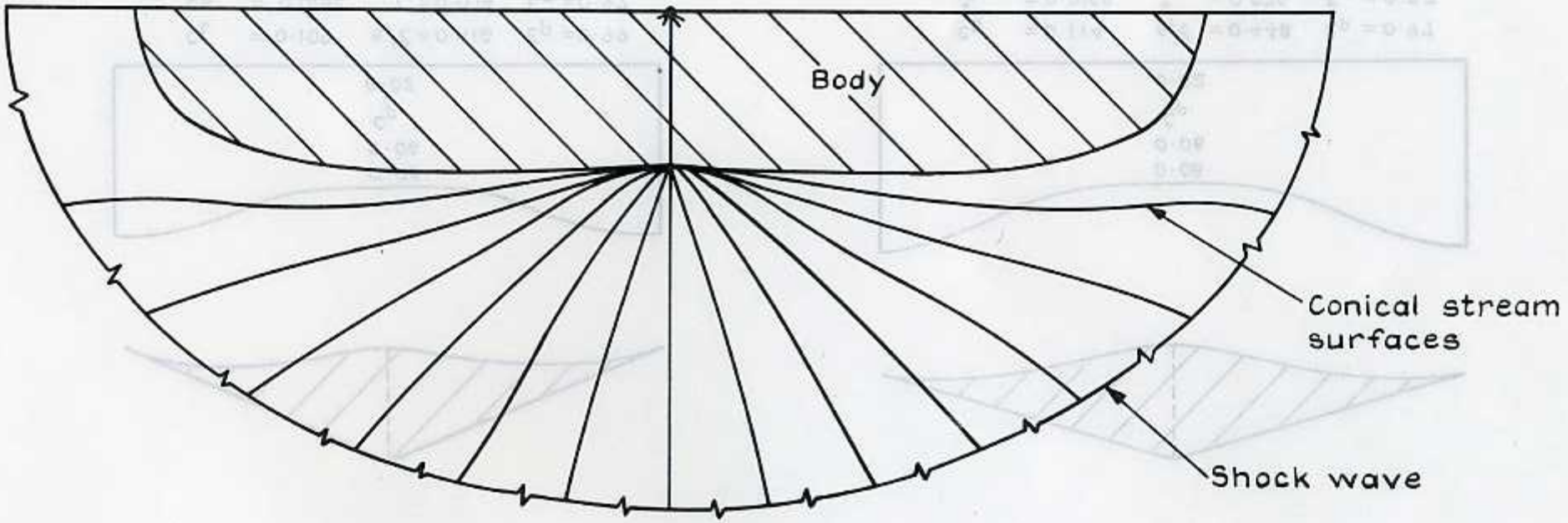

Fig. 7a Section through the flow behind an elliptic shock wave ($M_\infty = 4$)

$C_L = 0{\cdot}047$ $s/\ell = 0{\cdot}065$ $E_p = 0{\cdot}91$
$C_D = 0{\cdot}0040$ $\tau = 0{\cdot}110$ $E_\tau = 1{\cdot}00$
$L/D_p = 11{\cdot}9$ $S_w/S = 3{\cdot}42$

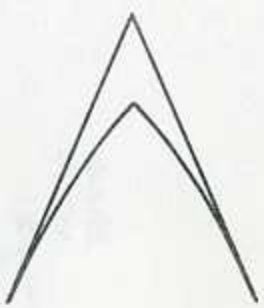

$C_L = 0{\cdot}049$ $s/\ell = 0{\cdot}130$ $E_p = 1{\cdot}01$
$C_D = 0{\cdot}0038$ $\tau = 0{\cdot}072$ $E_\tau = 1{\cdot}00$
$L/D_p = 12{\cdot}9$ $S_w/S = 1{\cdot}83$

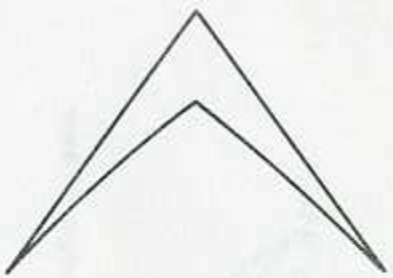

$C_L = 0{\cdot}051$ $s/\ell = 0{\cdot}197$ $E_p = 1{\cdot}03$
$C_D = 0{\cdot}0040$ $\tau = 0{\cdot}060$ $E_\tau = 1{\cdot}00$
$L/D_p = 12{\cdot}7$ $S_w/S = 1{\cdot}35$

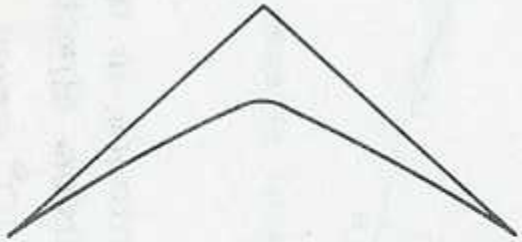

$C_L = 0{\cdot}054$ $s/\ell = 0{\cdot}264$ $E_p = 1{\cdot}03$
$C_D = 0{\cdot}0040$ $\tau = 0{\cdot}055$ $E_\tau = 1{\cdot}01$
$L/D_p = 12{\cdot}0$ $S_w/S = 1{\cdot}14$

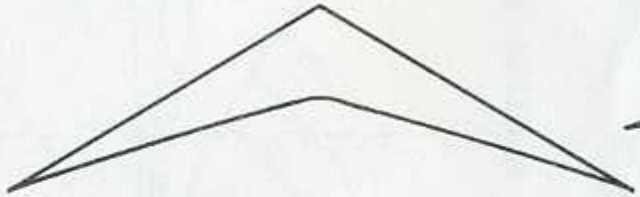

$C_L = 0{\cdot}060$ $s/\ell = 0{\cdot}327$ $E_p = 1{\cdot}06$
$C_D = 0{\cdot}0053$ $\tau = 0{\cdot}053$ $E_\tau = 1{\cdot}02$
$L/D_p = 11{\cdot}3$ $S_w/S = 1{\cdot}06$

$C_L = 0{\cdot}069$ $s/\ell = 0{\cdot}380$ $E_p = 0{\cdot}99$
$C_D = 0{\cdot}073$ $\tau = 0{\cdot}057$ $E_\tau = 0{\cdot}99$
$L/D_p = 9{\cdot}4$ $S_w/S = 1{\cdot}03$

Fig. 7b Wings with conical compression surfaces from the flow in Fig. 7a and streamwise upper surfaces

Fig. 7b

Fig. 8 a & b

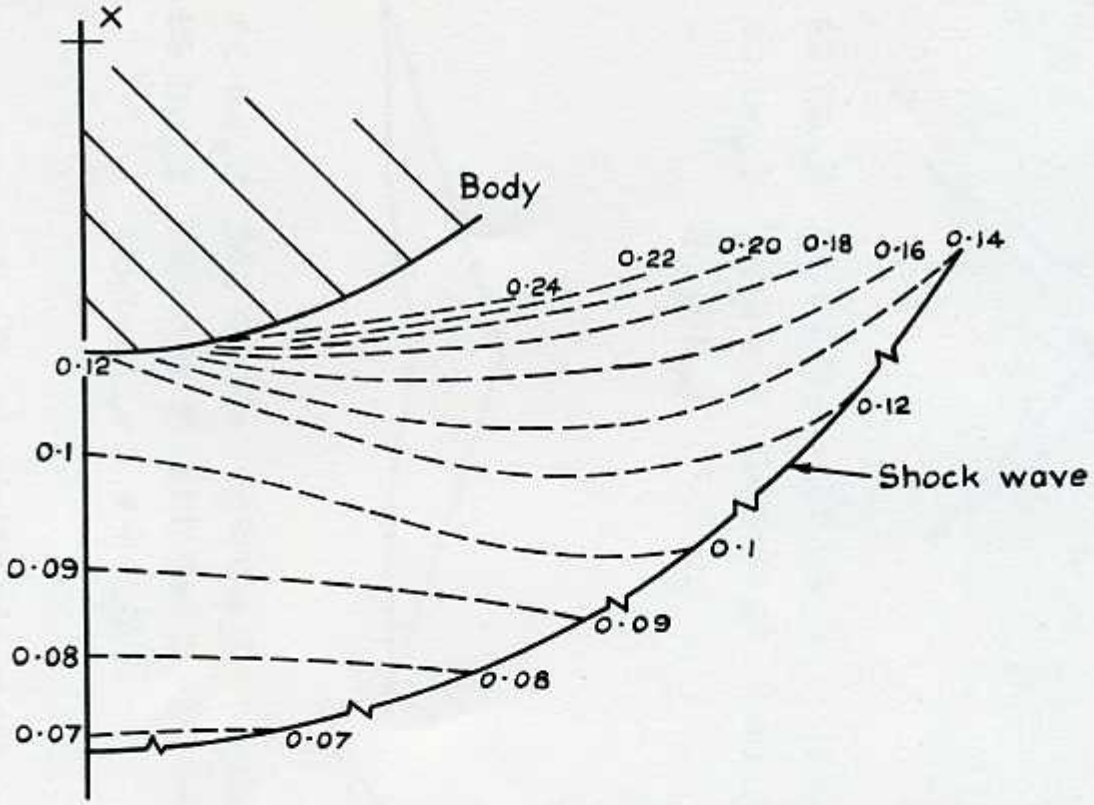

a Lift function contours in base plane

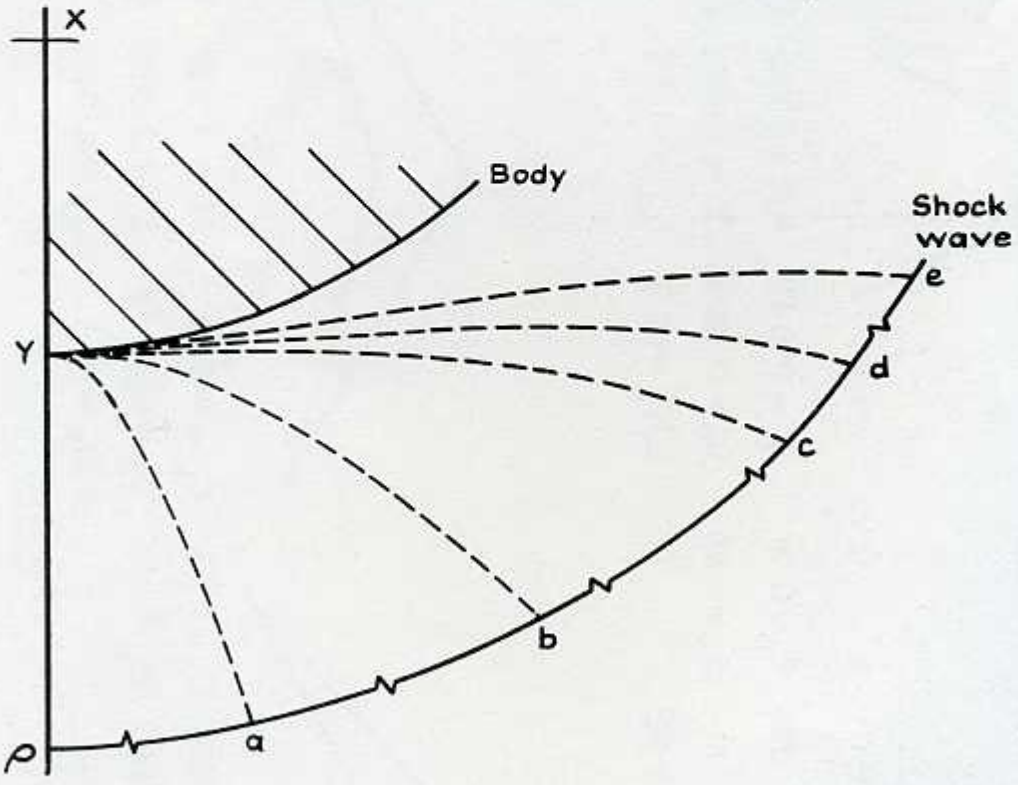

b Conical stream surfaces in base plane

Fig. 8 a & b Contours in a plane perpendicular to the free stream direction, for the flow about a 10° yawed cone at M=3·53

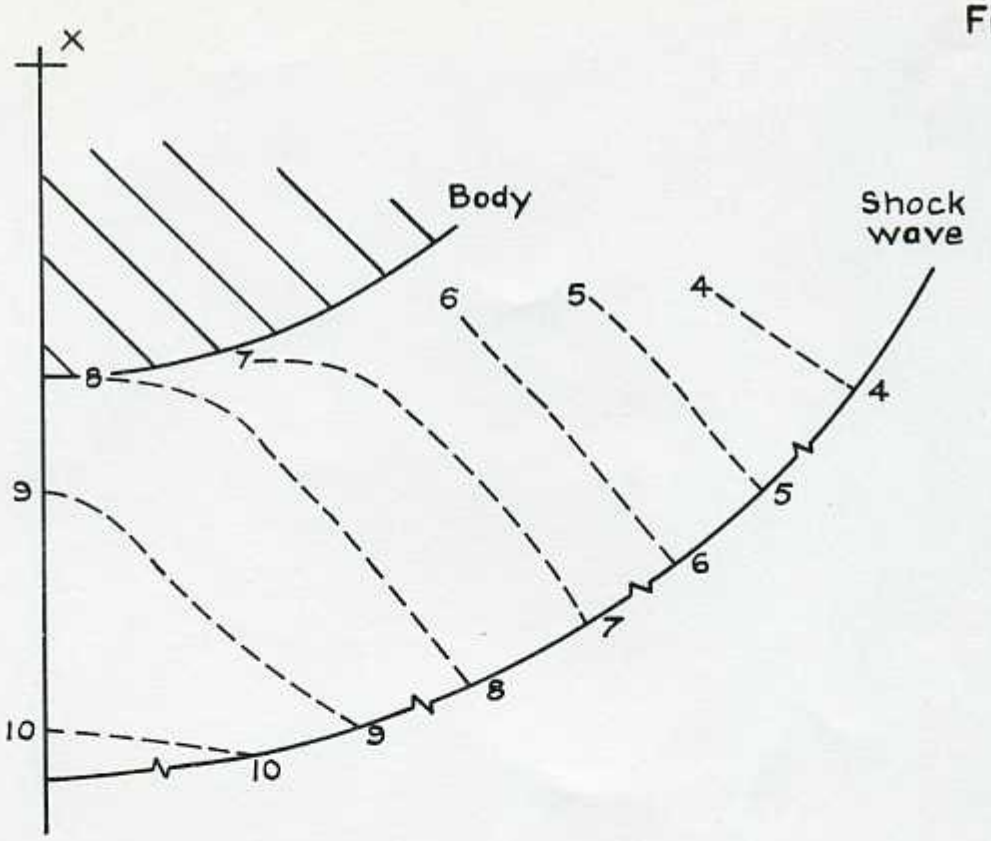

c Lift function over drag function contours in base plane

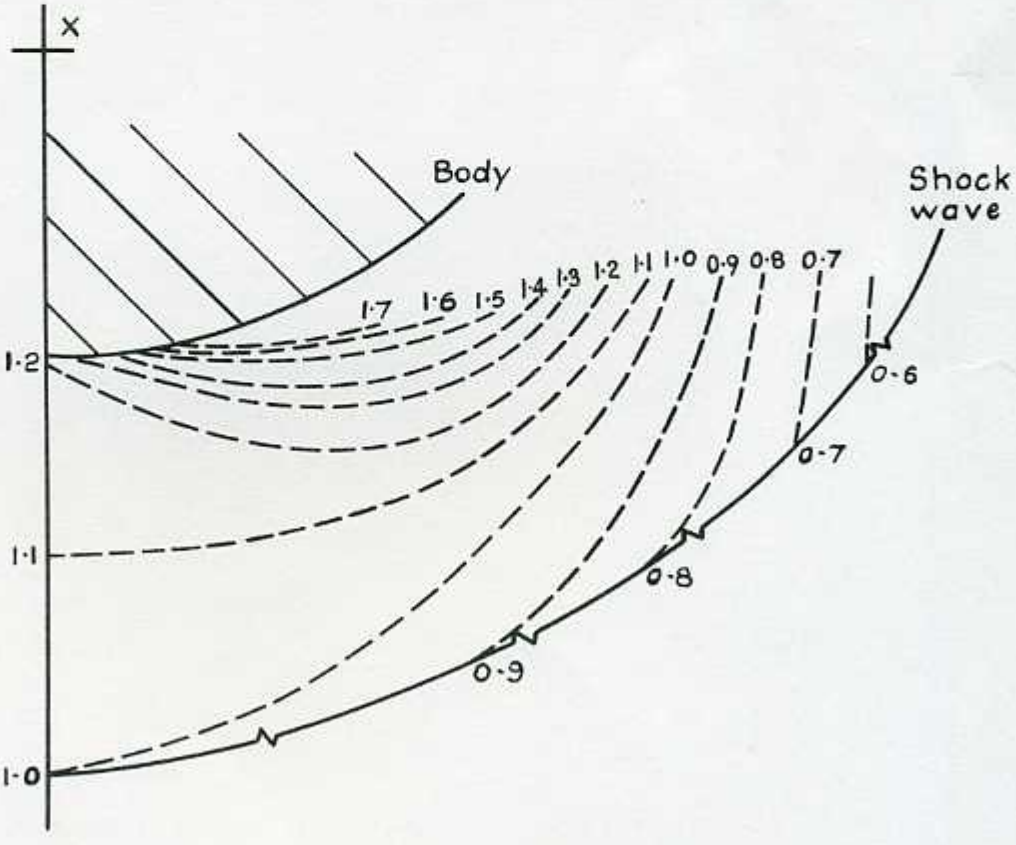

d E contours in base plane

Fig. 8 c & d Contours in a plane perpendicular to the free stream direction, for the flow about a 10° yawed cone at M=3·53